

MIT Open Access Articles

*Storm time observations of plasmasphere erosion
flux in the magnetosphere and ionosphere*

The MIT Faculty has made this article openly available. **Please share**
how this access benefits you. Your story matters.

Citation: Foster, J. C., P. J. Erickson, A. J. Coster, S. Thaller, J. Tao, J. R. Wygant, and J. W. Bonnell. "Storm Time Observations of Plasmasphere Erosion Flux in the Magnetosphere and Ionosphere." *Geophysical Research Letters* 41, no. 3 (February 11, 2014): 762–768

As Published: <http://dx.doi.org/10.1002/2013GL059124>

Publisher: American Geophysical Union (AGU)

Persistent URL: <http://hdl.handle.net/1721.1/109279>

Version: Final published version: final published article, as it appeared in a journal, conference proceedings, or other formally published context

Terms of Use: Article is made available in accordance with the publisher's policy and may be subject to US copyright law. Please refer to the publisher's site for terms of use.





RESEARCH LETTER

10.1002/2013GL059124

Special Section:

Early Results from the Van Allen Probes

Key Points:

- High-altitude plasmasphere erosion flux has significant magnitude
- Plasmasphere erosion flux has similar low- and high-altitude characteristics
- Fluence of ions through cusp and midnight sector exceeds $5E25$ ions s^{-1}

Correspondence to:

P. J. Erickson,
pje@haystack.mit.edu

Citation:

Foster, J. C., P. J. Erickson, A. J. Coster, S. Thaller, J. Tao, J. R. Wygant, and J. W. Bonnell (2014), Storm time observations of plasmasphere erosion flux in the magnetosphere and ionosphere, *Geophys. Res. Lett.*, *41*, 762–768, doi:10.1002/2013GL059124.

Received 27 DEC 2013

Accepted 13 JAN 2014

Accepted article online 16 JAN 2014

Published online 11 FEB 2014

Storm time observations of plasmasphere erosion flux in the magnetosphere and ionosphere

J. C. Foster¹, P. J. Erickson¹, A. J. Coster¹, S. Thaller², J. Tao³, J. R. Wygant², and J. W. Bonnell³

¹Haystack Observatory, Massachusetts Institute of Technology, Westford, Massachusetts, USA, ²Department of Physics and Astronomy, University of Minnesota, Twin Cities, Minneapolis, Minnesota, USA, ³Space Sciences Laboratory, University of California, Berkeley, California, USA

Abstract Plasmasphere erosion carries cold dense plasma of ionospheric origin in a storm-enhanced density plume extending from dusk toward and through the noontime cusp and dayside magnetopause and back across polar latitudes in a polar tongue of ionization. We examine dusk sector (20 MLT) plasmasphere erosion during the 17 March 2013 storm ($Dst \sim -130$ nT) using simultaneous, magnetically aligned direct sunward ion flux observations at high altitude by Van Allen Probes RBSP-A (at ~ 3.0 Re) and at ionospheric heights (~ 840 km) by DMSP F-18. Plasma erosion occurs at both high and low altitudes where the subauroral polarization stream flow overlaps the outer plasmasphere. At ~ 20 UT, RBSP-A observed $\sim 1.2E12$ $m^{-2} s^{-1}$ erosion flux, while DMSP F-18 observed $\sim 2E13$ $m^{-2} s^{-1}$ sunward flux. We find close similarities at high and low altitudes between the erosion plume in both invariant latitude spatial extent and plasma characteristics.

1. Introduction

Earth's ionosphere is produced by photodissociation of neutral atmosphere constituents by solar EUV photons. Under typical quiet conditions, upward diffusion along magnetic field lines populates higher altitudes with lighter ions (H^+ and He^+), and heavier species (O^+ , NO^+) settle to altitudes below ~ 1000 km. At low and middle latitudes, the ionosphere and overlying plasmasphere tend toward a state of diffusive equilibrium with nearly full flux tubes corotating with the Earth. At higher latitudes, however, solar wind driven magnetospheric circulation effects move plasma across field lines, and the result is a pronounced decrease in flux tube content with increasing latitude at low altitudes across the plasmasphere boundary layer (PBL) [Carpenter and Lemaire, 2004]. During disturbed magnetospheric conditions ionospheric O^+ is enhanced in the outer plasmasphere and energized O^+ ions are observed in the magnetospheric cusp, magnetotail lobes, nightside plasma sheet, and ring current. An understanding of the redistribution and energization of this ionospheric heavy ion material within the coupled ionosphere-plasmasphere-magnetosphere system is essential in the study of geospace storm processes and system response.

Incoherent scatter radar observations reveal plumes of ionospheric storm-enhanced density (SED; primarily O^+) extending from the dusk sector PBL to the vicinity of the noontime cusp [Foster, 1993]. Two-dimensional spatial snapshots of ionosphere-plasmasphere total electron content (TEC) frequently observe such SED plumes, with direct mapping along magnetic field lines to the plasmasphere erosion plumes seen in space-based plasmaspheric imagery by e.g., Imager for Magnetopause-to-Aurora Global Exploration (IMAGE) EUV [Foster et al., 2002]. Ionospheric radar observations within SED features show that the O^+ ionospheric plasma is streaming along the direction of the plume at velocities of 500 to > 2000 m/s, carrying significant ion fluxes of $\sim 1.0E14$ $m^{-2} s^{-1}$ into the F region cusp ionosphere [Foster et al., 2004; Erickson et al., 2011]. Combined radar and in situ DMSP satellite [Strom and Iwanaga, 2005] observations reveal that these sunward directed fluxes at ionospheric heights result from the overlap of the ring current driven subauroral polarization stream (SAPS) Foster and Vo [2002] with field lines threading the outer plasmasphere [Foster et al., 2007]. Nishimura et al. [2008] investigated SAPS in the outer plasmasphere using in situ measurements with CRRES electric field and plasma instruments in comparison with lower altitude DMSP observations in the topside ionosphere. They conclude, as suggested by Foster et al. [2007], that the SAPS electric field extends into the plasmasphere, and the plasmaspheric plasma close to the plasmopause drifts sunward, where it is expected to contribute to the formation of plasma plumes.

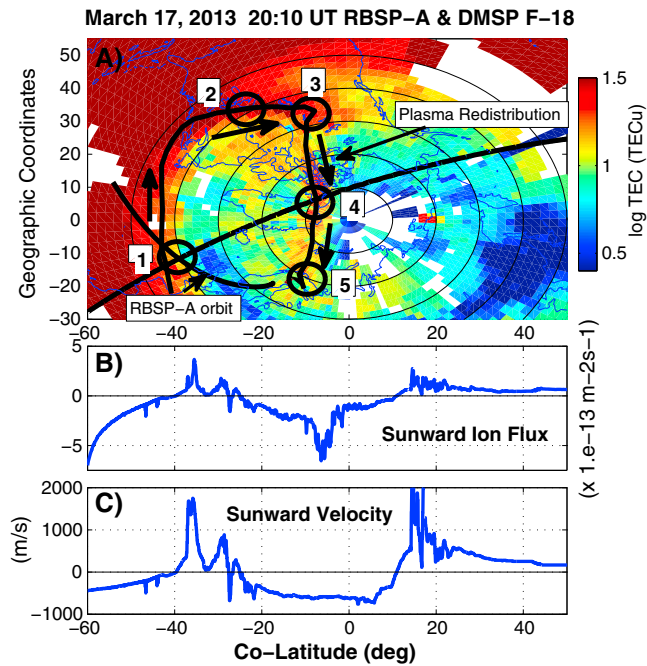


Figure 1. (a) GPS TEC snapshot of north polar regions (noon at the top, polar geographic coordinates) at 20:10 UT. Heavy black curves depict the magnetic footprints of RBSP-A and DMSP F-18 orbits, intersecting in the dusk sector PBL at ~20 MLT. (b) Ion flux (positive sunward) determined as the product of DMSP cross-track velocity and in situ (840 km altitude) ion density along the DMSP orbital track shown in Figure 1a. (c) Cross-track ion velocity (positive sunward) observed with the ion drift meter on DMSP F-18 along the orbital track displayed in Figure 1a.

For cold plasmas originating in the outer plasmasphere, $E \times B$ redistribution keeps both low-altitude (F region O^+) and high-altitude (topside H^+) ions on the same flux tube as they are convected from the PBL to cusp field lines, where dayside merging brings them into the polar cap [e.g., Zhang et al., 2013]. At lower altitudes, this large-scale plasma redistribution results in an elevated TEC polar tongue of ionization (TOI) extending antisunward across polar latitudes to the nightside auroral oval [Foster et al., 2005; Thomas et al., 2013].

2. Event Overview

In August 2012, the two Van Allen Probes spacecraft (RBSP A and B) [Stratton et al., 2012] were launched into elliptical orbits providing 10 to 12 PBL crossings each day. In this paper, we examine dusk sector (20 MLT) plasmasphere erosion processes, using simultaneous in situ observations of sunward ion flux both at high altitude (~3.0 Re) in the PBL by RBSP A and B, and at ionospheric heights (~840 km) by DMSP spacecraft. With temporally coincident global TEC measurements (GPS TEC) and ion flux observations both in the postnoon SED plume (Millstone Hill incoherent scatter radar) and in the polar TOI (DMSP), we provide a comprehensive snapshot of plasmasphere-ionosphere erosion and redistribution during the early recovery phase of the 17 March 2013 geomagnetic storm.

During the 17 March 2013 storm (Dst min = -132 nT), Van Allen Probes and DMSP spacecraft had a number of closely aligned magnetic field coincidences. Figure 1 presents a GPS TEC snapshot of north polar regions (noon at the top, polar geographic coordinates) at 20:10 UT. Figure 1 (heavy black curves) depicts the magnetic footprints of RBSP-A and DMSP F-18 orbits, intersecting in the dusk sector PBL at ~20 MLT. In situ DMSP observations of cross-track ion velocity (positive sunward) and ion flux, calculated as the product of velocity and ion density, are presented below the TEC map, plotted against colatitude to match the cross-polar orbital track shown above. The clear signature of SAPS sunward flow (~1700 m/s) is seen at the intersection point of the DMSP and RBSP-A orbital positions. The DMSP plasma instrument also observes the TOI embedded in the ~600 m/s antisunward convection region in the center of the polar cap.

The markings on Figure 1 indicate five principal regions involved in ionosphere-plasmasphere plasma redistribution. In the dusk sector (1) SAPS, coupling the ring current to the underlying subauroral ionosphere, erodes the

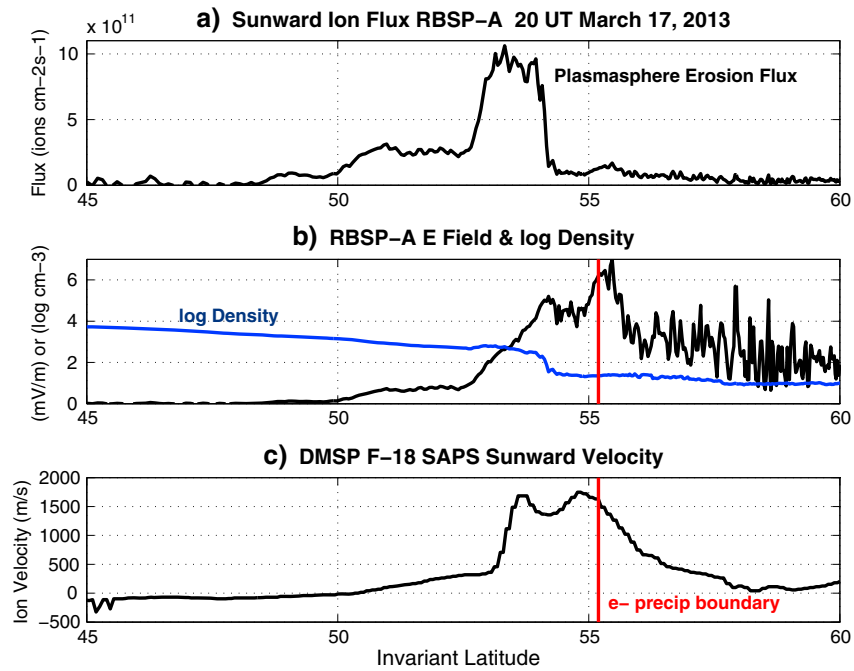


Figure 2. (a) Plasmasphere erosion flux derived from in situ observations as RBSP-A exited the outer plasmasphere near the apex of the $L = 3$ Re field line on 17 March 2013. Sunward flux is calculated as the product of density and $E \times B$ velocity. (b) EFW radial electric field magnitude and log electron density at ~ 20 UT on 17 March 2013. Sunward erosion flux maximizes ($\sim 1.2E13 \text{ m}^{-2} \text{ s}^{-1}$) in the region where the SAPS electric field overlaps the outer plasmasphere. (c) DMSP F-18 sunward ion velocity at ~ 830 km altitude, showing close similarity in position and shape with the outer plasmasphere SAPS EFW electric field. The red fiducial line indicates the equatorward extent of DMSP observed precipitation of 100 eV plasma sheet electrons.

outer plasmasphere. We investigate the erosion flux in this region in Figure 2 below. The SED/plasmasphere erosion plume (2) is carried in the SAPS flow channel from the PBL to the ionospheric cusp (3) and at high altitudes to the dayside magnetopause. Merging at (3) carries plasma, seen at lower altitudes as the TOI (4), onto field lines linking the polar cap and the magnetospheric tail lobe. Finally, antisunward flow in the TOI carries the eroded material into the midnight auroral oval (5) along field lines involved in nightside reconnection and particle energization. In this study, we investigate plasma redistribution observations during the recovery phase of the 17 March 2013 event in regions (1), (2), and (4). In a related paper [Foster et al., 2014], we discuss nightside observations in region (5) associated with a strong substorm and relativistic particle energization event observed by the Van Allen Probes spacecraft at apogee (5.7 Re) in the midnight sector late on 17 March. As has been described from IMAGE EUV observations [e.g., Goldstein and Sandel, 2005], storm time plasmasphere losses often begin with a strong sunward surge which carries outer plasmasphere material to the dayside magnetopause. Such a sunward surge was seen early in the 17 March 2013 event and could have accounted for an initial significant loss of plasmaspheric material across the contracted magnetopause.

3. Ionosphere and Plasmasphere Erosion Fluxes

Observations during the spatial/temporal coincidence of RBSP-A and DMSP F-18 described above are presented in Figure 2. The Van Allen Probes spacecraft carry a full complement of electron and ion instruments covering thermal (1 eV) to multi-MeV energies, electric and magnetic field sensors, and high-resolution wave instruments. Figure 2b shows the spatial variation of in situ plasma density (log scale) and radial electric field magnitude estimated from despun measurements by the Electric Field and Waves (EFW) [Wygant et al., 2013] sensors on RBSP-A, as the spacecraft exited the plasmasphere and crossed the near-equatorial PBL. Data are plotted versus invariant latitude as calculated in the RBSP ephemeris using the Tsyganenko dynamic field model [Tsyganenko and Sitnov, 2005]. For this interval, the RBSP-A spin axis (modified geocentric solar ecliptic (MGSE) x) is almost perpendicular to B and we calculate $|E| = (\text{sqrt}(E_y^2 + E_z^2))$ from measurements in the (MGSE y, z) plane assuming that E is purely radial and accounting for a combination of spacecraft position and spin

axis-pointing angle geometry. Our assumption of radial E is in agreement with past studies [e.g., Foster *et al.*, 2005; Nishimura *et al.*, 2008] that found the SAPS electric field at ~ 55 – 60 invariant latitude (inflat) to be entirely radial in the magnetosphere/meridional in the ionosphere.

In the outer plasmasphere, plasma density increased between 52° – 53° invariant and then decreased sharply by a factor of ~ 50 . Electric field intensity in the high-altitude SAPS region increased across the same region of outer plasmasphere density increase, reaching 3 – 5 mV/m in the 2° – 3° wide sunward SAPS flow region. We combine the EFW radial electric field measurements with in situ magnetic field magnitude from the EMFISIS magnetometer [Kletzing *et al.*, 2012] to calculate plasma flow velocity. RBSP-A in situ observation of the plasmasphere erosion flux ($\sim 1.2E12$ m $^{-2}$ s $^{-1}$ at 53.5 inflat) is plotted (Figure 2a) as the product of density (~ 600 cm $^{-3}$) and velocity (~ 2000 m/s). The spatial distribution of the SAPS sunward flow velocity observed by the ion drift meter on DMSP F-18 (Figure 2c) displays a close correspondence to the latitudinal width and structure of the electric field magnitude observed at high altitude (Figure 2b). We attribute the small ($< 1^\circ$) offset between invariant latitude positions of electric field features to disturbance related magnetic perturbations deviating slightly from the Tsyganenko model calculations used in the DMSP and Van Allen Probes spacecraft ephemeris calculations. The 5 mV/m magnitude of the electric field observed at RBSP-A maps to 55 mV/m $|E|$ at DMSP altitude, comparing very favorably with the 57 mV/m $|E|$ derived for the DMSP sunward velocity observations. Topside ionospheric erosion flux observed by DMSP F-18 at 840 km altitude (not shown) was $\sim 2.0E13$ m $^{-2}$ s $^{-1}$. Figures 2b and 2c (red fiducial lines) indicate the equatorward boundary of 100 eV electron precipitation observed by DMSP F-18.

For comparison, earlier in the event at $\sim 09:50$ UT, during an interval of strong disturbance activity several hours after storm onset, RBSP-B crossed the dusk sector erosion plume at 21 MLT observing a ~ 7 mV/m $|E|$, velocity ~ 3200 m/s, and sunward plasma flux $\sim 6.5E12$ m $^{-2}$ s $^{-1}$. RBSP-B $|E|$ mapped to the ~ 840 km DMSP altitude was ~ 70 mV/m. Although not a direct field-aligned spatial/temporal coincidence, DMSP F-17 crossed the SAPS channel at $\sim 09:30$ UT in the Southern Hemisphere at 18.5 MLT observing ionospheric velocity ~ 1800 m/s, $|E| \sim 70$ mV/m, and sunward ionospheric flux of $\sim 2.4 E14$ m $^{-2}$ s $^{-1}$.

Previous SED plume and sunward ionospheric flux observations in region (2) have been performed primarily with the Millstone Hill incoherent scatter radar combined with DMSP satellite overflights of the SAPS/SED region. For the 17 March event, the Millstone Hill radar was performing wide field scans of ionospheric plasma parameters across the SAPS channel at $\sim 90^\circ$ W longitude and 14 MLT at the time of the observations presented in Figures 1 and 2. In Figure 3a, we present F region westward velocity across the PBL. The location and $\sim 5^\circ$ latitude extent of the SAPS flow is indicated. The 600 – 800 m/s SAPS westward velocity observed is typical for this MLT compared to the statistical study of Erickson *et al.* [2011]. By integrating the radar electron density observations, we are able to reconstruct the F region TEC (total electron content between 100 km and 800 km altitude), and in Figure 3b we compare this with the simultaneously observed GPS vertical TEC (~ 100 km to 4 Re altitude) along the same longitude. F region TEC is $\sim 40\%$ of the total TEC below 60° invariant latitude, increases to $\sim 65\%$ between 60° and 62° invariant in the SED region and then drops sharply poleward of 62° invariant latitude. Sunward flux in the SED reaches $1.5E14$ m $^{-2}$ s $^{-1}$ as the postnoon F region O^+ plasma is carried toward the cusp.

4. Polar Cap TOI Plasma Dynamics

As shown in Figure 1, the DMSP F-18 orbital track crossed the TOI (region (4)) in the center of the polar cap. The spacecraft measured in situ antisunward $\sim 6.0E13$ m $^{-2}$ s $^{-1}$ ion flux at ~ 840 km altitude in the TOI at $\sim 20:15$ UT. In Figure 4, we investigate variability of TOI total electron content for the 17 March event. Examining GPS north polar TEC map data (e.g., Figure 1) at 5 min temporal resolution, we observe patches of enhanced TEC entering polar latitudes from the position of the ionospheric cusp (region (3)) intermittently throughout the event. GPS TEC data are calculated on a $1^\circ \times 1^\circ$ geodetic latitude/longitude grid, with each pixel independently calculated as the median of all determinations of vertical TEC intersecting that pixel at 350 km altitude [Rideout and Coster, 2006]. On 17 March, TEC data were obtained during each 5 min interval in an average of 250 such spatially distributed pixels at geodetic latitudes $> 80^\circ$. In Figure 4, we plot the median value of TEC observed above 80° north latitude at each 5 min period for the 3 day interval 16 – 18 March 2013.

Baker *et al.* [2014] describe the 17 March 2013 storm in the context of the overall evolution of radiation belt particle populations. Storm onset occurred at $\sim 06:00$ UT on 17 March (indicated in Figure 4, red vertical line). At

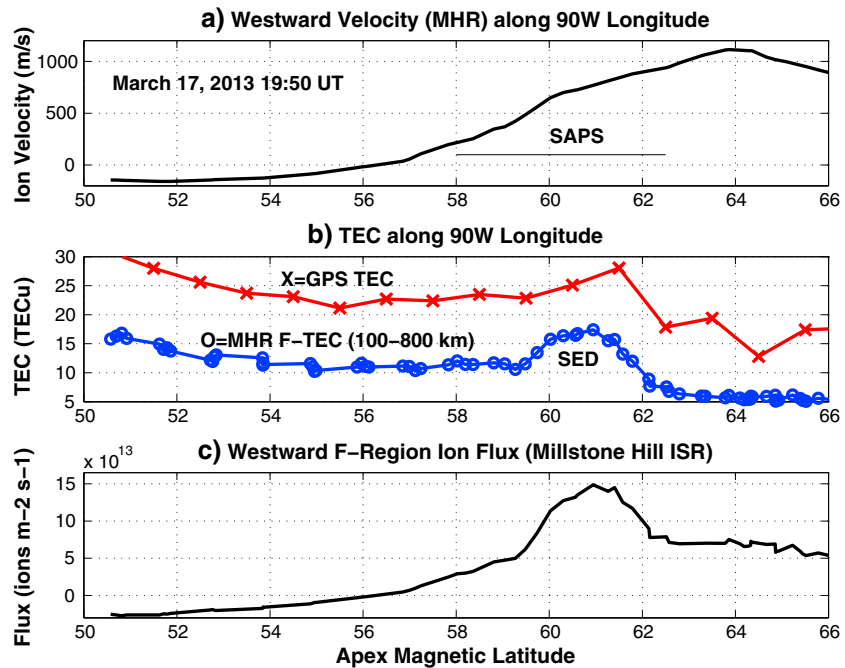


Figure 3. Millstone Hill ionospheric radar observation of (a) SAPS flow velocity and (b) *F* region TEC along the 90°W longitude meridian at ~14 MLT at the time of the GPS TEC, RBSP-A and DMSP observations shown in Figures 1 and 2. (c) Sunward ion flux ($1.5E14 \text{ m}^{-2} \text{ s}^{-1}$ maximum value within the SED plume at 60°–62° invariant latitude) is shown. GPS TEC (ground to ~4 Re altitude), measured along 90°W longitude, is shown in red. *F* region TEC accounts for ~40% of the total TEC below 59° invariant latitude, and ~65% of the total TEC within the SED erosion plume.

that time, a pronounced increase in polar cap TEC magnitude is evident, continuing sporadically until ~22:17 UT on 17 March, at which time there is a clear and sudden decrease in north polar TOI. As described in a companion paper [Foster *et al.*, 2014], a strong substorm (*AE* index ~1000 nT) and magnetospheric reconfiguration occurred at this time, ending the active phase of the storm, followed by a significant energization of the nightside and radiation belt particle populations.

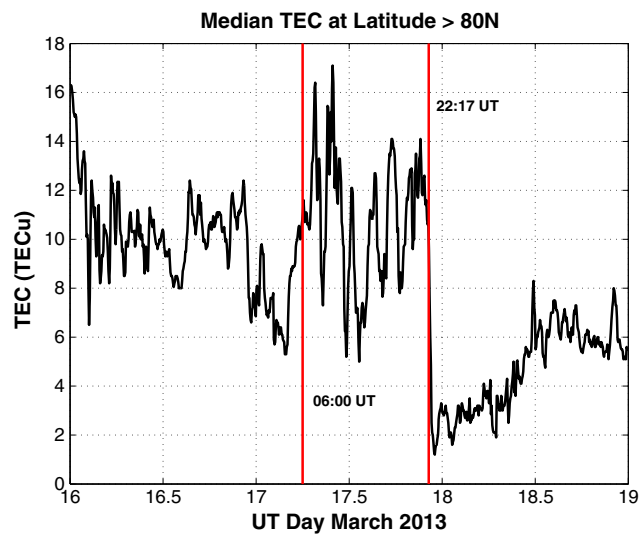


Figure 4. North polar TOI intensity and variation, plotted as 5 min median values of all independent GPS TEC observations at latitudes above 80°N. Red lines indicate the times of storm onset and the 22:17 UT substorm event in the recovery phase of the storm. We interpret the intermittent transfer of dayside SED plasma across cusp field lines into the polar TOI as a low-altitude signature of dayside merging activity at the magnetopause.

As suggested by *Foster and Doupnik* [1984] and placed in a global geospace context by *Foster* [2008], we interpret the intermittent transfer of dayside SED plasma across cusp field lines and into the polar cap as a low-altitude signature of dayside merging activity at the magnetopause. Examining solar wind parameters for an event with polar cap TEC signatures similar to 17 March 2013, *Zhang et al.* [2013] have concluded that enhancements and decreases of the TOI fluxes entering polar latitudes are related to the onset and cessation of dayside merging.

For the time shown in Figure 1, we estimate the total fluence of eroded ionospheric/plasmaspheric ions carried antisunward in the TOI channel to be $\sim 5. \text{E}25 \text{ s}^{-1}$. This value combines the column density observed by GPS TEC ($\sim 15 \text{E}16 \text{ m}^{-2}$) with the DMSP antisunward velocity ($\sim 600 \text{ m s}^{-1}$) and the spatial width of the TOI observed along the DMSP orbit ($\sim 6.3 \text{E}5 \text{ m}$). We perform a similar calculation of the ion fluence in the SED/erosion plume that carries the eroded plasmasphere material toward the cusp. Combining the Millstone Hill Radar sunward velocities and the GPS TEC, as presented in Figure 3, we calculate the sunward fluence across the 5° span $57.5\text{--}62.5$ latitude to be $\sim 7 \text{E}25 \text{ s}^{-1}$ which compares well with the $5. \text{E}25 \text{ s}^{-1}$ antisunward fluence observed at that time in the TOI.

The long duration of the TOI flux on 17 March 2013 suggests that high-latitude midnight sector field lines were richly populated with plasmaspheric material prior to the 22:17 UT substorm event. Detailed Van Allen Probes and ground-based observations during that substorm and their contribution to the energization of MeV radiation belt electrons are discussed in the companion paper by *Foster et al.* [2014].

5. Ionospheric Plasma Redistribution Processes

Plasmasphere erosion carries cold dense plasma of ionospheric origin toward the noontime cusp and dayside magnetopause. GPS TEC mapping shows the ionospheric footprint of this process as a continuous plume of storm enhanced density (SED) extending from the dusk sector into and through the daytime cusp region and back across polar latitudes in a polar cap tongue of ionization. This circulation provides an enhanced source of ionospheric ions for injection into the magnetosphere, energization in the nighttime plasma sheet, and injection into the inner magnetosphere in the storm time ring current. The 17 March event provides quantitative, simultaneous evidence at multiple points within this redistribution chain that significant plasma erosion fluxes are involved both at ionospheric and magnetospheric altitudes.

Acknowledgments

We thank G. Wilson for making DMSP data available for this study. Work with the Van Allen Probes observations at MIT Haystack Observatory was supported by a subaward from the University of Minnesota to the Massachusetts Institute of Technology. Radar operations and GPS TEC analysis activities are supported by a cooperative agreement between the National Science Foundation and the Massachusetts Institute of Technology.

The Editor thanks Dennis Gallagher and an anonymous reviewer for their assistance in evaluating this paper.

References

- Baker, D. N., et al. (2014), Gradual diffusion and punctuated phase space density enhancements of highly relativistic electrons: Van Allen Probes observations, *Geophys. Res. Lett.*, *41*, doi:10.1002/2013GL058942.
- Carpenter, D., and J. Lemaire (2004), The plasmasphere boundary layer, *Ann. Geophys.*, *22*, 4291–4298.
- Erickson, P. J., F. Beroz, and M. Z. Miskin (2011), Statistical characterization of the American sector subauroral polarization stream using incoherent scatter radar, *J. Geophys. Res.*, *116*, A00J21, doi:10.1029/2010JA015738.
- Foster, J. C. (1993), Storm-time plasma transport at middle and high latitudes, *J. Geophys. Res.*, *98*, 1675–1689.
- Foster, J. C. (2008), Ionospheric-magnetospheric-heliospheric coupling: Storm-time thermal plasma redistribution, in *Mid-Latitude Dynamics and Disturbances*, *Geophys. Monograph Ser.*, vol. 181, edited by P. M. Kintner et al., pp. 121–134, AGU, Washington, D. C., doi:10.1029/181GM12.
- Foster, J. C., and J. R. Doupnik (1984), Plasma convection in the vicinity of the dayside cleft, *J. Geophys. Res.*, *89*, 9107–9113.
- Foster, J. C., and H. B. Vo (2002), Average characteristics and activity dependence of the subauroral polarization stream, *J. Geophys. Res.*, *107*(A12), 1475, doi:10.1029/2002JA009409.
- Foster, J. C., P. J. Erickson, A. J. Coster, J. Goldstein, and F. J. Rich (2002), Ionospheric signatures of plasmaspheric tails, *Geophys. Res. Lett.*, *29*(13), 1623, doi:10.1029/2002GL015067.
- Foster, J. C., A. J. Coster, P. J. Erickson, F. J. Rich, and B. R. Sandel (2004), Stormtime observations of the flux of plasmaspheric ions to the dayside cusp/magnetopause, *Geophys. Res. Lett.*, *31*, L08809, doi:10.1029/2004GL020082.
- Foster, J. C., et al. (2005), Multiradar observations of the polar tongue of ionization, *J. Geophys. Res.*, *110*, A09531, doi:10.1029/2004JA010928.
- Foster, J. C., W. Rideout, B. Sandel, W. T. Forrester, and F. J. Rich (2007), On the relationship of SAPS to storm-enhanced density, *J. Atmos. Space Terr. Phys.*, *69*, 303–313.
- Foster, J. C., et al. (2014), Prompt energization of relativistic and highly relativistic electrons during a substorm interval: Van Allen Probes observations, *Geophys. Res. Lett.*, *41*, doi:10.1002/2013GL058438.
- Goldstein, J., and B. R. Sandel (2005), The global pattern of evolution of plasmaspheric drainage plumes, in *Inner Magnetosphere Interactions: New Perspectives from Imaging*, *Geophys. Monogr. Ser.*, vol. 159, edited by J. Burch and M. Schultz, pp. 1–22, AGU, Washington, D. C., doi:10.1029/159GM02.
- Kletzing, C. A., et al. (2012), The electric and magnetic field instrument and integrated science (EMFISIS) on RBSP, *Space Sci. Rev.*, *179*(1–4), 127–181, doi:10.1007/s11214-013-9993-6.
- Nishimura, Y., J. Wygant, T. Ono, M. Iizima, A. Kumamoto, D. Brautigams, and R. Friedel (2008), SAPS measurements around the magnetic equator by CRRES, *Geophys. Res. Lett.*, *35*, L10104, doi:10.1029/2008GL033970.
- Rideout, W., and A. Coster (2006), Automated GPS processing for global total electron content data, *GPS Solutions*, *10*, 219–228.

- Stratton, J. M., R. J. Harvey, and G. A. Heyler (2012), Mission overview for the Radiation Belt Storm Probes mission, *Space Sci. Rev.*, doi:10.1007/s11214-012-9933-x.
- Strom, S. R., and G. Iwanaga (2005), Overview and history of the Defense Meteorological Satellite Program, "Crosslink", *Aerosp. Corp. Mag. Adv. Aerosp. Technol.*, 6(1), 11–15.
- Thomas, E. G., J. B. H. Baker, J. M. Ruohoniemi, L. B. N. Clausen, A. J. Coster, J. C. Foster, and P. J. Erickson (2013), Direct observations of the role of convection electric field in the formation of a polar tongue of ionization from storm enhanced density, *J. Geophys. Res. Space Physics*, 118, 1180–1189, doi:10.1002/gra.50116.
- Tsyganenko, N. A., and M. I. Sitnov (2005), Modeling the dynamics of the inner magnetosphere during strong geomagnetic storms, *J. Geophys. Res.*, 110, A03208, doi:10.1029/2004JA010798.
- Wygant, J. R., et al. (2013), The Electric Field and Waves (EFW) instruments on the Radiation Belt Storm Probes mission, *Space Sci. Rev.*, doi:10.1007/s1124-013-0013-7.
- Zhang, Q. H., et al. (2013), Direct observations of the evolution of polar cap ionization patches, *Science*, 339(6127), 1597–1600, doi:10.1126/science.1231487.